Conductivity, dielectric relaxation, and viscosity of ternary microemulsions: The role of the experimental path and the point of view of percolation theory

J. Peyrelasse and C. Boned
Laboratoire de Physique des Matériaux Industriels, Centre Universitaire de Recherche Scientifique, Université de Pau et des Pays de l'Adour, Avenue de l'Université, 64000 Pau, France
(Received 24 May 1989)

The results obtained for the conductivity, dielectric relaxation, and viscosity of ternary water-AOT-oil microemulsions are presented and discussed in the context of percolation theory. [Here, AOT is an abbreviation for sodium bis(2-ethylhexyl) sulfosuccinate.] Several parameters are considered: the volume fraction ϕ(water + AOT), the molar ratio n = [water]/[AOT], the temperature, the salt content of the aqueous solution, and the nature of the oil. Certain results obtained by replacing the water with glycerol (waterless microemulsion) are reported. Eight different experimental paths were systematically followed. At constant temperature and salt content we have the paths n = const, ϕ = const, P_w = const (water content by weight), P_o = const (oil content by weight), P_s = const [surfactant (AOT) content by weight], $P_S/(P_S+P_o)$ = const (i.e., P_S/P_o = const). We also considered variations of temperature and salt content for constant values of all the other parameters. The experimental curves have various different shapes for conductivity, dielectric permittivity, relaxation frequency, or viscosity. Depending on the path followed we observed either monotonic variations or, in contrast, curves presenting maxima and minima. Discussion of the results in connection with percolation theory and the concept of "percolation threshold lines" [M. Moha-Ouchane, J. Peyrelasse, and C. Boned, Phys. Rev. A **35**, 3027 (1987)] is satisfactory and the theoretical curves are comparable in all respects with the experimental curves. Finally, in the Discussion, certain analogies of behavior (and therefore of interpretation) are emphasized between the microemulsions studied here and certain quaternary systems.

INTRODUCTION

Microemulsions are systems that have been very widely studied by a number of authors over the last few years because of their fundamental importance and their practical applications. A microemulsion is a macroscopically single-phase system that is generally the result of the mutual solubilization of water and oil. This mutual solubility requires the addition of one or several surface agents. The resulting systems have four or five components (after addition of a surfactant, a cosurfactant, and possibly salt), which makes analysis of the experimental results difficult. It is not always necessary to add a cosurfactant to obtain a microemulsion. It has been known for some time that sodium bis(2-ethylhexyl) sulfosuccinate (AOT) allows a high level of solubilization of oil and water without the addition of another component being required. The result is a ternary system that is easier to study. Surfactants other than AOT have this property. Equally, detergent-free systems have been presented as being water-in-oil–type microemulsions;[1,2] for example, the water–2-propanol–n-hexane system. It is also possible[3–7] to prepare waterless microemulsions by replacing the water with liquids such as formamide, glycerol, etc. Here too by choosing a suitable surfactant a ternary system can be produced: for example, the methanol-AOT-cyclohexane system[4] was one of the first to be quoted in the literature.

For water-in-oil microemulsions, when the volume fraction of water or temperature increases, a rapid increase in electrical conductivity (of several decades) can be observed in certain cases.[8–18] Several investigations[13,17,19] appear to confirm the idea that this is a dynamic percolation phenomenon,[10,19] which implies the formation of clusters of water droplets in the continuous medium. When the drops are sufficiently close to each other, effective transfer of charge carriers may take place.[20] Similarly, the dielectric behavior of these systems can be interpreted with the same percolation model[13,14,16,21–24] that explains why a maximum of static permittivity and a minimum[22] of the characteristic frequency of the dielectric relaxation are associated with the percolation threshold. Similar behavior has been observed[25] for waterless microemulsions of the glycerol-AOT-isooctane type. It should be pointed out that for waterless microemulsions the percolation phenomenon has already been mentioned[26] as regards conductivity.

Dynamic viscosity was also discussed in connection with the percolation phenomenon for ternary water-AOT-oil systems[27–29] and for (water + NaCl)–toluene–dodecyl sulfate sodium–butanol systems when the salt content in the microemulsion varies.[30] The phenomenon can also be observed for waterless microemulsions of the glycerol-AOT-isooctane type.[25]

For ternary water-AOT-oil systems a systematic study[18,22,28] has been carried out throughout the phase diagram for conductivity, dielectric relaxation, and viscosity. This study investigates the influence of the

volume fraction in dispersed matter (water +AOT), of the molar ratio $n=[H_2O]/[AOT]$, of the temperature, of the salt content, and of the nature of the oil. The work led to the development of the concept of "percolation threshold lines in the ternary diagram." In order to study a microemulsion by varying its characteristics, an experimental path in the ternary diagram is generally chosen. For example, $n=$const might be imposed, or the temperature might be varied while all the other parameters are fixed. Also, the salt content might be varied, or a constant weight ratio $P_{\text{surfactant}}/P_{\text{oil}}$ might be selected, and so on. A consequence of the concept of percolation threshold lines is that, according to the experimental path followed, the shapes of the experimental curves can be very different because they depend on the position of the line in the ternary diagram relative to the path followed, and because they also depend on any deformation that the line might undergo with varying temperature. The experimental curve may, in some cases, have a very unusual shape. For instance, if the path is appropriately chosen, adding water to the water-AOT-oil microemulsion causes a reduction in conductivity. The same is true of adding salt. In previous papers we mentioned this consequence of percolation threshold lines without explicitly developing the possibilities this approach can offer. In the present paper we will be developing these aspects and showing that analysis in terms of percolation, based on the percolation threshold lines, leads to the interpretation of several unusual results. We will also see that it raises doubts, at least partially, about further interpretations[31–34] concerning the measurements we made previously on similar systems, interpretations which have been reported in the literature and that should consequently be reassessed in the light of our new knowledge of the subject.

BACKGROUND TO THE PHENOMENON OF PERCOLATION IN MICROEMULSIONS

The determination of complex permittivity ϵ^* of heteregeneous systems is a well-known problem which has for some time been the subject of a great number of investigations. From a very general point of view the complex permittivity ϵ^* of a heterogeneous binary system may be represented by a relationship of the form $\epsilon^*=G(\epsilon_1^*,\epsilon_2^*,\phi,p_k)$ in which ϵ_1^* and ϵ_2^* are the complex permittivities of constituents 1 and 2, ϕ is, for example, the volume fraction of constituent 1, and p_k represents the parameters which enable the function G to contain all the information on the geometry of the dispersion and on the interactions which take place within the system. The models which enable an approximation of the function G are often based on effective or mean-field theories. Satisfactory results are generally obtained while the interactions within the mixture are weak, which is often the case when the volume function of one of the constituents is small, and as long as the dispersion can be considered macroscopically homogeneous. But when the dispersed particles are no longer isolated from each other, in other words, when clusters form, the conventional models no longer apply and the concept of percolation can be successfully used. The general relationship for complex permittivity[35,36] is

$$\frac{\epsilon^*}{\epsilon_1^*}=|\phi-\phi_c|^{\mu}f\left[\frac{\epsilon_2^*/\epsilon_1^*}{|\phi-\phi_c|^{(\mu+s)}}\right], \tag{1}$$

in which ϕ_c represents the volume fraction of constituent 1 at the percolation threshold and in which the exponents μ and s are positive. The function $f(z)$ in which z is a complex variable satisfies the following asymptotic forms:

$$\phi>\phi_c, |z|\ll 1, f(z)=c_1+c_1'z ,$$

$$\phi<\phi_c, |z|\ll 1, f(z)=c_2z ,$$

$$|z|\gg 1, \forall\phi, f(z)=cz^{\mu/(\mu+s)} .$$

If it is assumed that the two components are dielectric conductors of static permittivities ϵ_{1s} and ϵ_{2s} and conductivity σ_1 and σ_2 we obtain

$$\epsilon_1^*=\epsilon_{1s}-j\frac{\sigma_1}{\epsilon_0\omega}, \quad \epsilon_2^*=\epsilon_{2s}-j\frac{\sigma_2}{\epsilon_0\omega}, \quad \omega=2\pi\nu$$

in which ν is the frequency of the electric field applied, ϵ_0 is the dielectric permittivity of a vacuum and $j^2=-1$. The heterogeneous system built up from components 1 and 2 presents static permittivity ϵ_s and conductivity σ. We obtain the following.

(a) We have

$$\epsilon_s=c_2\epsilon_{2s}(\phi_c-\phi)^{-s}, \tag{2}$$

$$\sigma=c_2\sigma_2(\phi_c-\phi)^{-s}, \tag{3}$$

where $\phi<\phi_c, |z|\ll 1$.

(b) We have

$$\epsilon_s=c_1'\epsilon_{2s}(\phi-\phi_c)^{-s}\left[1+\frac{c_1}{c_1'}\frac{\epsilon_{1s}}{\epsilon_{2s}}(\phi-\phi_c)^{(\mu+s)}\right],$$

$$\sigma=c_1\sigma_1(\phi-\phi_c)^{\mu}\left[1+\frac{c_1'}{c_1}\frac{\sigma_2}{\sigma_1}(\phi-\phi_c)^{-(\mu+s)}\right],$$

where $\phi>\phi_c, |z|\ll 1$.

As $\mu+s$ is positive and $\epsilon_{1s}/\epsilon_{2s}$ does not tend towards infinity, while ϕ is sufficiently close to ϕ_c we have

$$\epsilon_s=c_1'\epsilon_{2s}(\phi-\phi_c)^{-s}. \tag{4}$$

So when ϕ is sufficiently close to ϕ_c, $\epsilon_s\propto|\phi-\phi_c|^{-s}$ on either side of ϕ_c. Moreover, if $\sigma_2/\sigma_1\ll 1$ (for example, with a perfect insulator $\sigma_2=0$), close to the percolation threshold one can still have

$$\sigma_2/\sigma_1\ll|\phi-\phi_c|^{(\mu+s)}$$

and one consequently obtains

$$\sigma=c_1\sigma_1(\phi-\phi_c)^{\mu}. \tag{5}$$

(c) Finally in line with a suggestion made by Bergman the dielectric relaxation of the system is characterized[37,38] by the relaxation frequency

$$\nu_R\propto|\phi-\phi_c|^{(\mu+s)}, \tag{6}$$

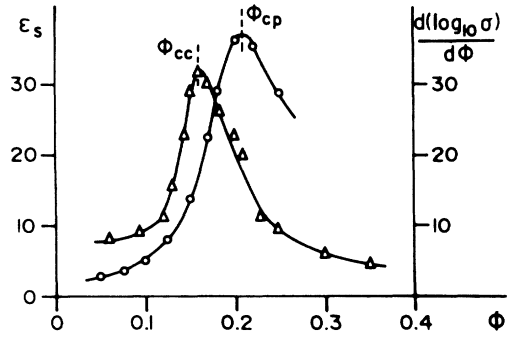

FIG. 1. Water-AOT-undecane system ($n=8$, $T=15\,^{\circ}C$). Variations of ϵ_s (○) and $d(\log_{10}\sigma)/d\phi$ (△) vs ϕ. (From Ref. 21).

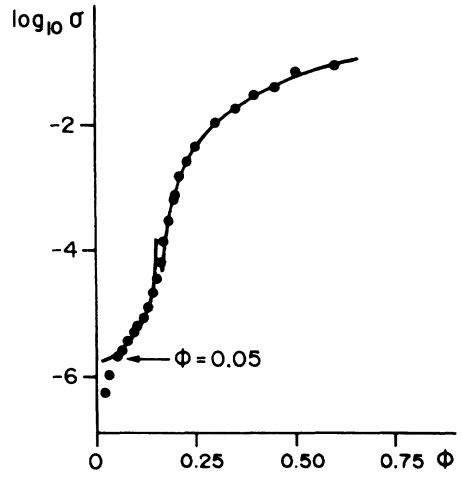

FIG. 3. Water-AOT-undecane system. Variations of the conductivity σ ($S\,m^{-1}$) vs volume fraction ϕ ($n=8$, $T=15\,^{\circ}C$). ——, theoretical curves [Eqs. (3) and (5)]; ●, experimental data. (From Ref. 17).

which is valid if ϕ is close to ϕ_c. So when $\phi \rightarrow \phi_c$ we have $\nu_R \rightarrow 0$.

In practice, a maximum of $(1/\sigma)(d\sigma/d\phi)$ and of ϵ_s is observed.[21] Figure 1 illustrates the result. The difference between the percolation threshold of conductivity ϕ_{cc} and the percolation threshold ϕ_{cp} of permittivity could be a result of the hopping phenomenon,[20,22] and has already been pointed out by other authors.[13] Similarly, Fig. 2 represents the variations of ν_R in the neighborhood of the percolation threshold. It will be noted that $\nu_R \rightarrow 0$ for ternary water-AOT-oil microemulsions[22,23,31] as well as for waterless glycerol-AOT-isooctane microemulsions.[25] It should therefore be stressed that Eqs. (3) and (5) which describe conductivity, Eqs. (2) and (4) which describe static permittivity, and Eq. (6) which describes the characteristic frequency of relaxation are only valid if $|z| \ll 1$, in other words, if $\sigma_2/\sigma_1 \ll 1$ and if ϕ is close to ϕ_c. In particular, it is impossible to use these laws at extremely small dilutions ($\phi \rightarrow 0$) or at unit concentration ($\phi \rightarrow 1$). Moreover, they cannot be used in the immediate vicinity of ϕ_c where in practice no discontinuity for ϵ_s and σ is observed. For example, for conductivity, a continuous transition between the values predicted by Eqs. (3) and (5) is observed. The transition interval can be defined[35] by

$$\Delta = \left[\frac{\sigma_2}{\sigma_1}\right]^{1/(\mu+s)}$$

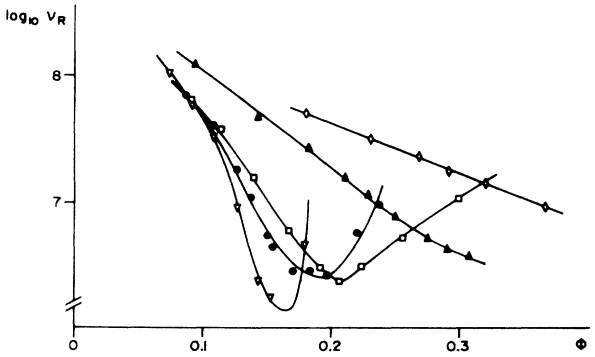

FIG. 2. Water-AOT-dodecane system. Variations of ν_R (Hz) vs ϕ for different values of n. ◇, 3.6; ▲, 4.4; □, 6; ●, 7; ▽, 10. (From Ref. 21).

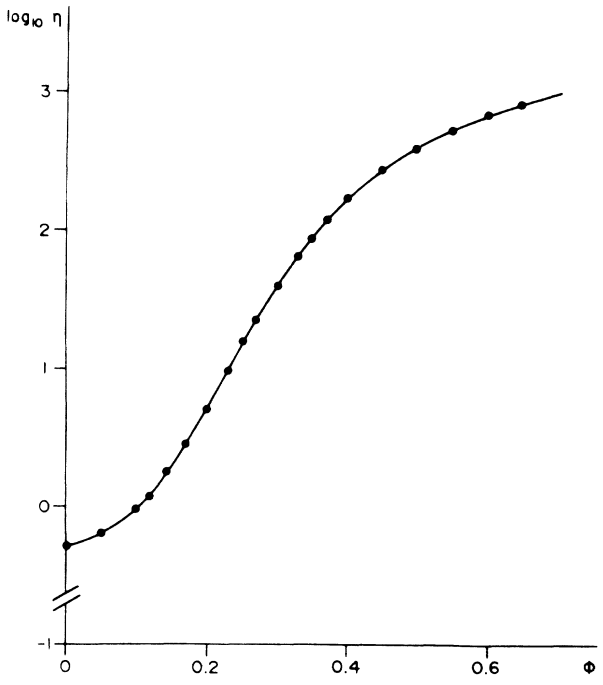

FIG. 4. Glycerol-AOT-isooctane system. Variations of the viscosity η (cP) vs volume fraction ϕ (n=[glycerol]/[AOT]=3.2, $T=25\,^{\circ}C$). (From Ref. 24).

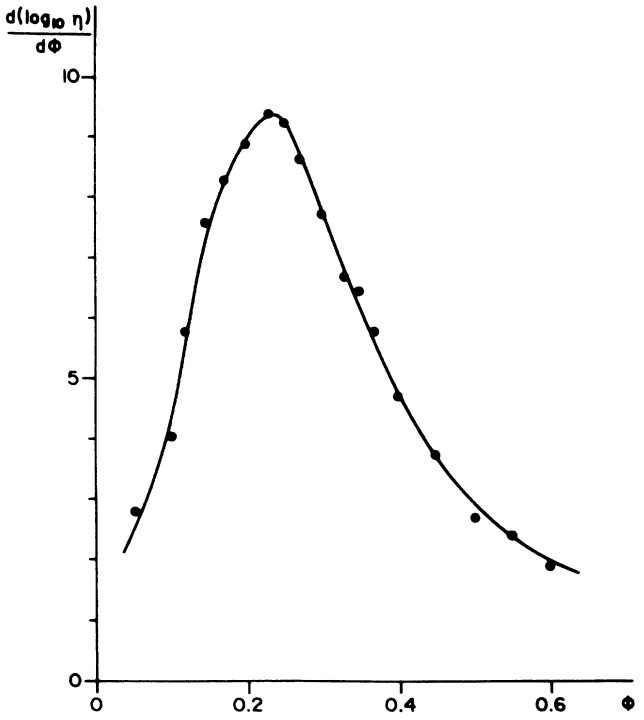

FIG. 5. Glycerol-AOT-isooctane system. Variations of $d(\log_{10}\eta)/d\phi$ vs volume fraction ϕ. (n=[glycerol]/[AOT]=3.2, T=25 °C). (From Ref. 24).

When $\sigma_2/\sigma_1 \ll 1$, Δ is small, and Eqs. (3) and (5) account for variations of σ with ϕ in very close proximity to the percolation threshold. This is, for instance, the case for the water-AOT-undecane system,[18] and Fig. 3 presents an example of this. It also shows that when one is too far from the threshold ($\phi < 0.05$) the equations do not apply. Figure 1 represents the corresponding variations of $d(\log_{10}\sigma)/d\phi$.

When the percolation threshold is present one might think that the viscosity η might also present particular variations. This has been observed not only for ternary microemulsions with water[27–30] but also for waterless ternary microemulsions.[25] In particular, the $(1/\eta)(d\eta/d\phi)$ curve also goes through a maximum at the percolation threshold. Viscosity has been less comprehensively studied in the context of percolation theory than has complex permittivity. However, by analogy[28] with the previous equations, one can write

$$\eta = c_2'' \eta_2 |\phi - \phi_c|^{-s'} \quad \text{if } \phi < \phi_c \tag{7}$$

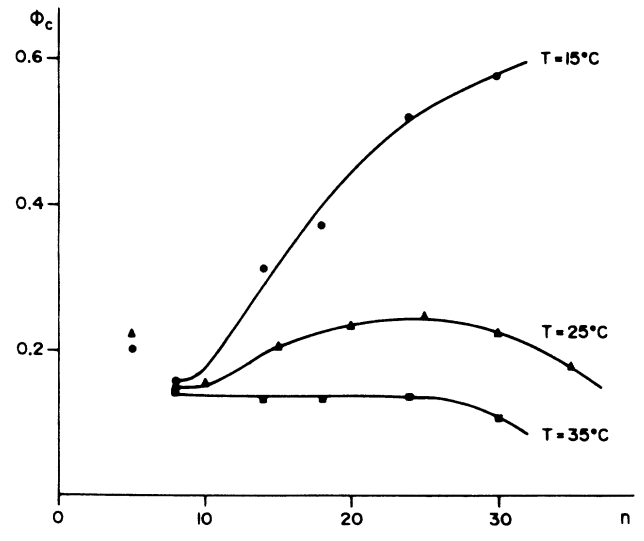

FIG. 6. Water-AOT-undecane system. Variations of the percolation threshold ϕ_c vs n. ●, T=15°C; ▲, T=25 °C; ■, T=35 °C. (From Ref. 17).

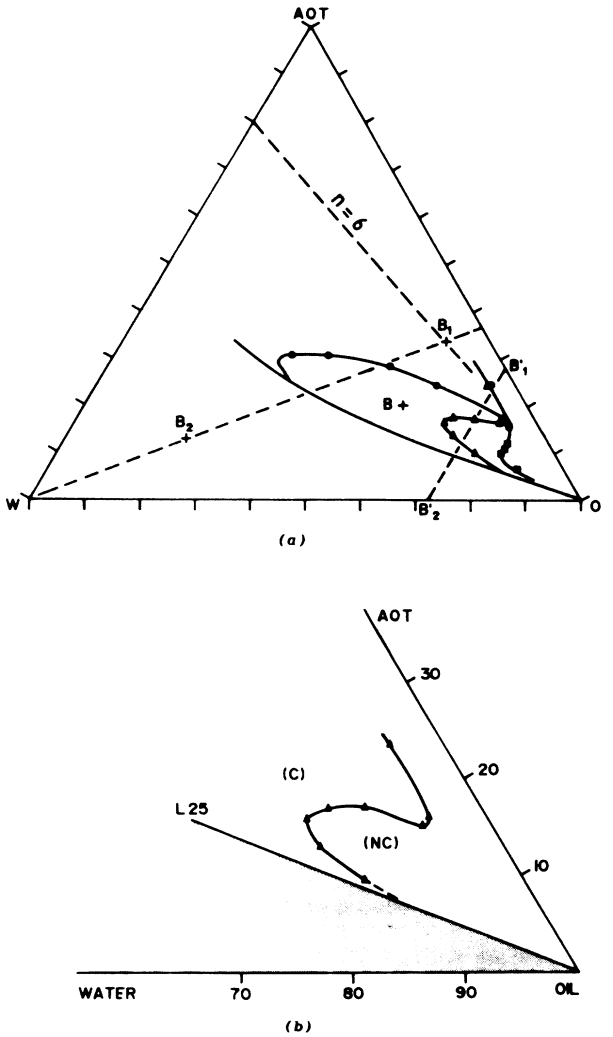

FIG. 7. Water-AOT-undecane system. (From Ref. 17). (a) Lines of the percolation thresholds in the ternary diagram (weight fraction). ●, T=15°C; ▲, T=25 °C; ■, T=35 °C; (b) Line of the percolation thresholds in the ternary diagram (weight fraction) at T=25 °C. L25, boundary of the monophasic area at T=25 °C. (C), conductive area; (NC), nonconductive area.

$$\eta = c_1'' \eta_1 |\phi - \phi_c|^{\mu'} \quad \text{if } \phi > \phi_c \ , \tag{8}$$

in which s' and μ' are two positive exponents, η_1 and η_2 the viscosities of constituents 1 and 2, and ϕ the volume fraction of constituent 1.

Figures 4 and 5 are characteristic. By extrapolating the theoretical considerations concerning conductivity to the case of dynamic viscosity one can assume that Eqs. (7) and (8) are valid only if $\eta_2/\eta_1 \ll 1$. In the case of water-in-oil microemulsions this condition is not satisfied. However $(1/\eta)(d\eta/d\phi)$ presents a maximum which corresponds to the percolation threshold as determined from the conductivity curves.[28] In the case of glycerol-AOT-isooctane microemulsions (Figs. 4 and 5) the situation is much more favorable. This is clear from the fact that the $\eta^{-1/1.2}(\phi < \phi_c)$ and $\eta^{1/1.94}(\phi > \phi_c)$ curves, plotted against ϕ, are found to be two straight lines which intersect on the ϕ axis, at the percolation threshold.[25] This also shows that the exponents s' and μ' of dynamic viscosity appear to be those which occur in the dynamic model of percolation of microemulsions ($s = s' = 1.2$ and $\mu = \mu' = 1.94$). This illustrates the general character of the phenomenon of dynamic percolation of microemulsions.

We determined[18] the position of the percolation threshold line in the ternary diagram for water-AOT-oil systems. To conclude this background presentation we present in Fig. 6 the variations of the threshold as a function of the molar ratio n for different temperatures in a system in which the oil is undecane, and Fig. 7 represents the position in the ternary diagram of the associated threshold lines. For Fig. 7(b), (C) is the conducting zone which corresponds to $\phi(\text{water} + \text{AOT}) > \phi_c$ and (NC) is the nonconducting zone which corresponds to $\phi < \phi_c$. Finally, it should be noted that an increase in the threshold value is observed with increasing salt content[18] or decreasing length of the oil chain,[22] consistent with a decrease in the interactions within the microemulsion.

EXPERIMENTAL TECHNIQUES

Systems studied. Having already carried out a study over the whole range of the ternary diagram for different conditions we used these existing experimental results.[18,22,25,28] We will above all be discussing the water-AOT-undecane system, but the conclusions that we will be presenting can be generalized without difficulty to cover the other systems studied. We will supply some examples.

We used cyclohexane (Fluka AG "free of benzene," for uv spectroscopy), iso-octane (Fluka AG puriss), undecane (Fluka AG purum), dodecane (Fluka AG purum), glycerol (Prolabo Rectapur), and AOT (Fluka AG purum). In a few cases we used aqueous solutions of sodium chloride (Prolabo Normapur). All the samples are characterized by the volume fraction ϕ (water or glycerol+AOT) and by the molar ratio $n = [\text{water}]/[\text{AOT}]$ (or $[\text{glycerol}]/[\text{AOT}]$). Temperature stabilization of the samples was performed to $\pm 0.1\,^{\circ}\text{C}$. For the study of the influence of salt we used p_s, the percentage of salt by weight in the brine solution. Finally, it should be noted that P_w, P_0, and P_S are the percentages by weight of water, oil, or surfactant in the microemulsion [Fig. 8(a)].

Techniques employed. The stationary electrical conductivity σ is measured using a Wayne Kerr B331 precision bridge which operates at frequency 1592 Hz. The measuring cell is a Philips-Mullard-type cell and is calibrated before use with aqueous solutions of KCl. Relative uncertainty for σ is estimated at 0.1%.

Measurement of relative viscosity was performed using a capillary viscosimeter (Viscotimer Lauda S/1). The specific gravity was measured with an automatic Anton Paar KG DMA 45 densimeter with an absolute uncertainty lower than 10^{-3} g/cm^3. Relative uncertainty for the dynamic viscosity is estimated at less than 0.5%.

To measure dielectric relaxation we used a time domain spectroscopy method. The development of our apparatus has been presented in two technical articles.[39,40] It consists of a Tektronix WP/200 system with a reflectometer and a digital processing oscilloscope, all of which are controlled by a computer. The relative accuracy for the real part ϵ' and the imaginary part ϵ'' ($\epsilon^* = \epsilon' - j\epsilon''$) is 3%. At frequencies less than 5 MHz a study of complex permittivity was carried out with a Hewlett Packard 4129 A impedancemeter, also computer controlled.

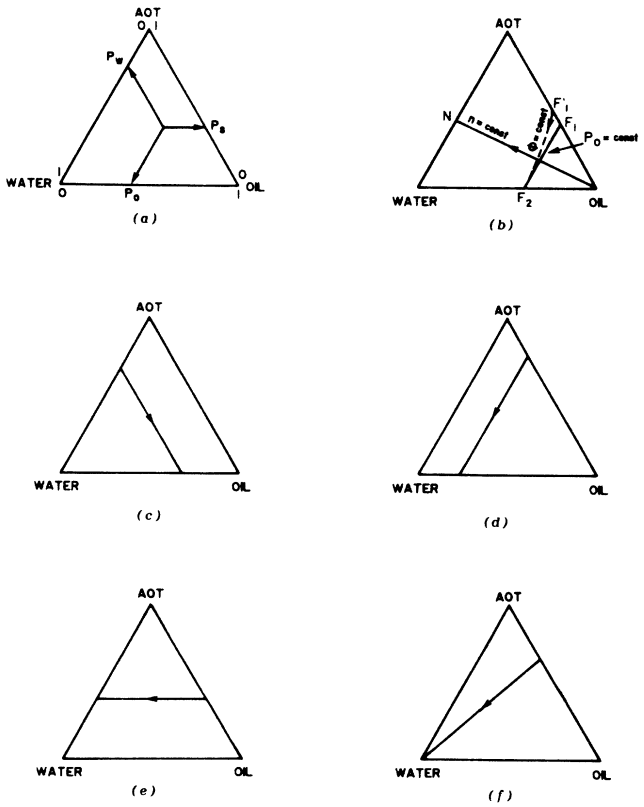

FIG. 8. Experimental ways. (a) Ponderal ternary diagram; (b) n=const and ϕ=const; (c) P_w=const; (d) P_0=const; (e) P_S=const; (f) P_o/P_S=const.

EXPERIMENTAL RESULTS

Experimental paths followed. In the ternary diagram the samples were initially investigated at T=const and n=const. Figure 8(b) shows the corresponding path in the ternary diagram be weight. We also carried out measurements at ϕ=const and variable n(T=const). When taken together, the two sets of curves can easily reconstitute by interpolation, the curves corresponding to the experimental paths P_w=const, P_o=const, P_S=const, and P_S/P_o=const at T=const [Figs. 8(c)–8(f)]. Figure 8(b) represents the path ϕ=const at T=const. Unlike the five preceding cases this does not provide a straight line in the ternary diagram by weight, but as the densities ρ_{AOT} and ρ_{water} (or $\rho_{glycerol}$) are not very different (ρ_{AOT}=1.135 g/cm^3 and $\rho_{glycerol}$=1.126 g/cm^3, for example, at 25 °C), this path is close to that followed at P_0=const [Fig. 8(d)]. The six preceding paths assume T=const but also p_s=const (salt content). All things being equal in regard to the other parameters we also performed experiments which correspond to the two supplementary paths: variable T or variable p_s. In all we will therefore be presenting results for eight different experimental paths. Let us remark at this point that it is well known that for the water-AOT-undecane system, at low or intermediate water concentrations, the microemulsion consists of water droplets in oil subjected to Brownian movement. These droplets interact[41,42] and these attractive interactions grow regularly with the molar ratio n, i.e., with the radius of the droplets. In the case of the glycerol-AOT-heptane system,[43] light scattering measurements show the existence of spherical droplets of glycerol stabilized by the surfactant, the size depending mainly on the molar ratio n. Consequently, at least for water-AOT-oil systems, of the eight experimental paths followed, only the path n=const [Fig. 8(b)] maintains constant radius and

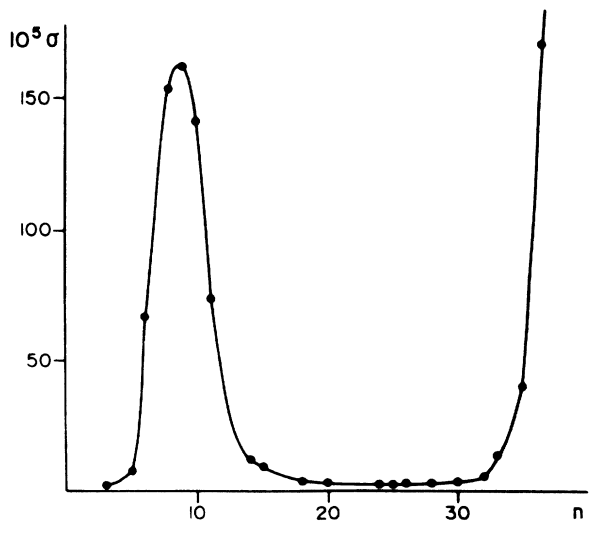

FIG. 9. Water-AOT-undecane system. Variations of the conductivity σ(S m^{-1}) vs n (ϕ=0.2, T=25 °C). (From Ref. 17).

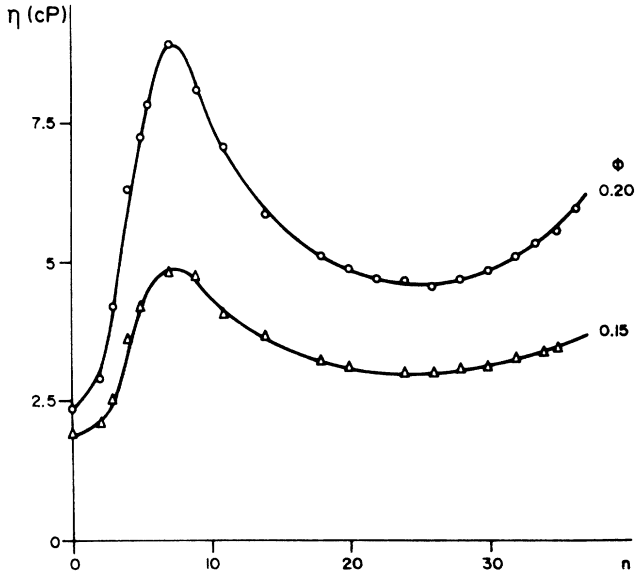

FIG. 10. Water-AOT-undecane system (T=25 °C). Variations of η (cP) vs n for different values of ϕ are shown. (From Ref. 27).

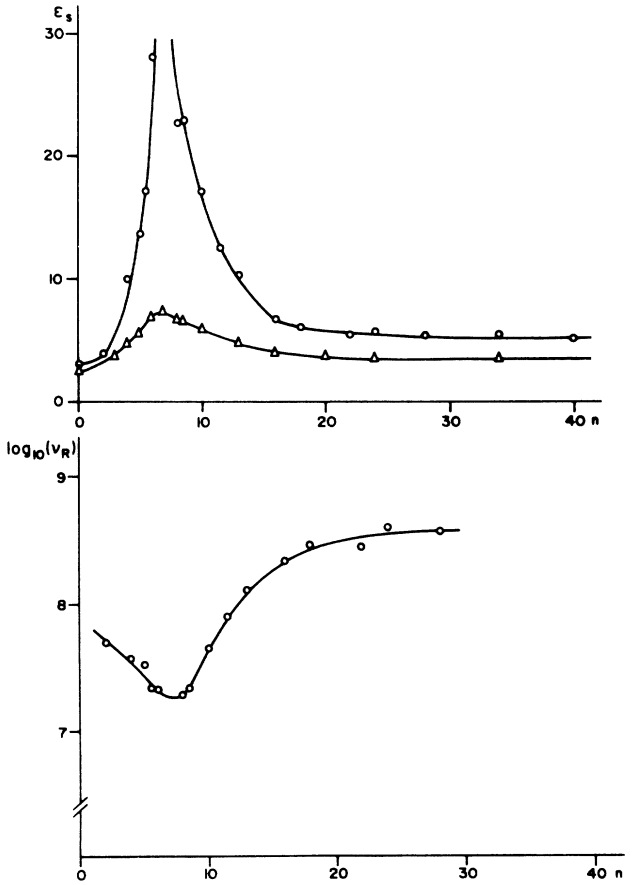

FIG. 11. Water-AOT-isooctane system (T=25 °C). Variations of ϵ_s (○; ϕ=0.3; △, ϕ=0.2) and ν_R (○, ϕ=0.3) vs n. (From Ref. 21). (ν_R in Hz).

interactions between droplets. It is this path which, by using the above-mentioned relationships, can determine the value of ϕ_c by means of numerical analysis. The value of ϕ_c depends mainly on the interactions and the reader may refer to the model developed by Bug *et al.*[44] and Safran.[20] For all the paths, at constant T and p_s the property studied depends on $\phi-\phi_c(n)$. (For conductivity we observed[18] that the prefactors remain practically constant with respect to n). With the exception of the path $n=$const, $\phi_c(n)$ varies when all the other paths are followed. It is this fact which makes it difficult to analyze the results if one has not previously determined the curve of variation of ϕ_c along the path followed, taking into account the corresponding variations of n.

Path $n=$const [Fig. 8(b)]. Figures 1–5, which were discussed above, are examples of experimental curves.

Path $\phi=$const [Fig. 8(b)]. Figures 9–11 represent the curves $\sigma(n)$, $\eta(n)$, $\epsilon_s(n)$, and $\nu_R(n)$ (characteristic relaxation frequency: frequency at the maximum of ϵ'' for water-AOT-oil systems) obtained for various ternary microemulsions. It is not easy to interpret them, at least at first, because of their complex shapes. Identical curves, with maxima and minima, have been obtained by Rouvière and co-workers[45–47] for water-AOT-(decane or heptane) systems.

Path $P_w=$const [Fig. 8(c)]. Figure 12 represents $\log_{10}\sigma=f(P_0)$ for the water-AOT-undecane system at $T=25\,^\circ$C. The curve presents a more or less pronounced minimum according to the selected value of P_w.

Path $P_o=$const [Fig. 8(d)]. Figure 13 represents the variations of $\log_{10}\sigma$ with P_w for different values of P_o in the case of the water-AOT-undecane system at $T=25\,^\circ$C. Each curve presents a maximum and a minimum. The latter becomes insignificant for low values of P_o.

Path $P_S=$const [Fig. 8(e)]. Figure 14(a) represents the variations of σ with P_w for different values of P_S in the case of the water-AOT-undecane system at $T=25\,^\circ$C. Figure 14(b) represents the variations of $\log_{10}\sigma$ with P_w, which show that there is a minimum and a maximum for the values $P_S=0.1$ and 0.2. They are not visible on the curve in 14(a) because of the scale of the representation.

Path $P_S/P_o=$const [Fig. 8(f)]. Figure 15(a) represents the variations of $\log_{10}\sigma$ with P_w for different values of P_S/P_o in the case of the water-AOT-undecane system at $T=25\,^\circ$C. There is a maximum and a minimum, which

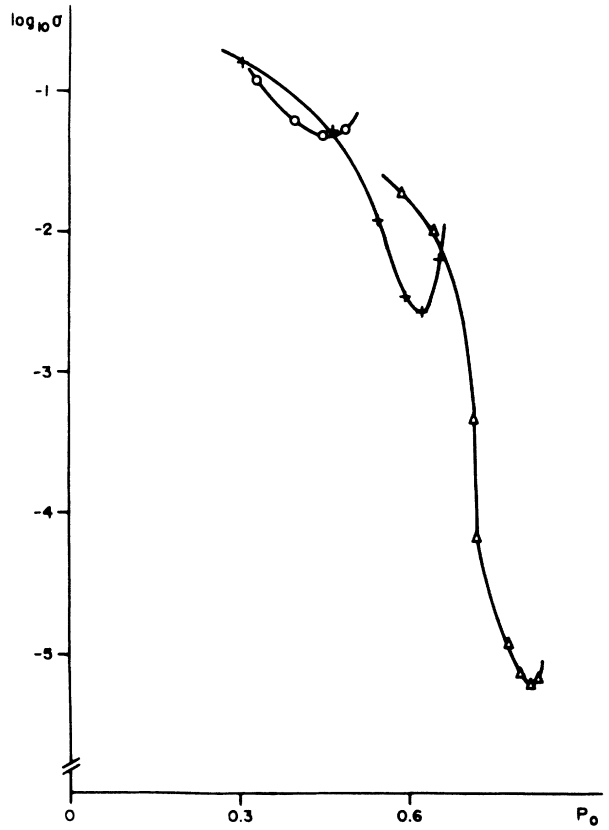

FIG. 12. Water-AOT-undecane system ($T=25\,^\circ$C). Experimental way $P_w=$const. Variations of $\log_{10}\sigma$ (○, $P_w=0.3$; +, $P_w=0.2$; △, $P_w=0.1$) vs P_o. (σ in S m^{-1}).

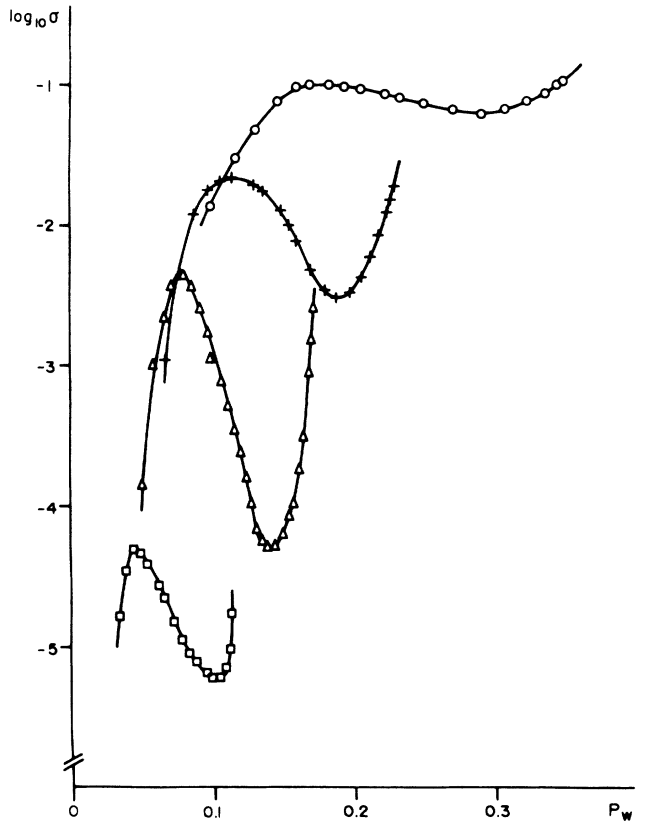

FIG. 13. Water-AOT-undecane system ($T=25\,^\circ$C). Experimental way $P_o=$const. Variations of $\log_{10}\sigma$ (○, $P_0=0.4$; +, $P_o=0.6$, △, $P_o=0.7$; □, $P_o=0.8$) vs P_w. (σ in S m^{-1}).

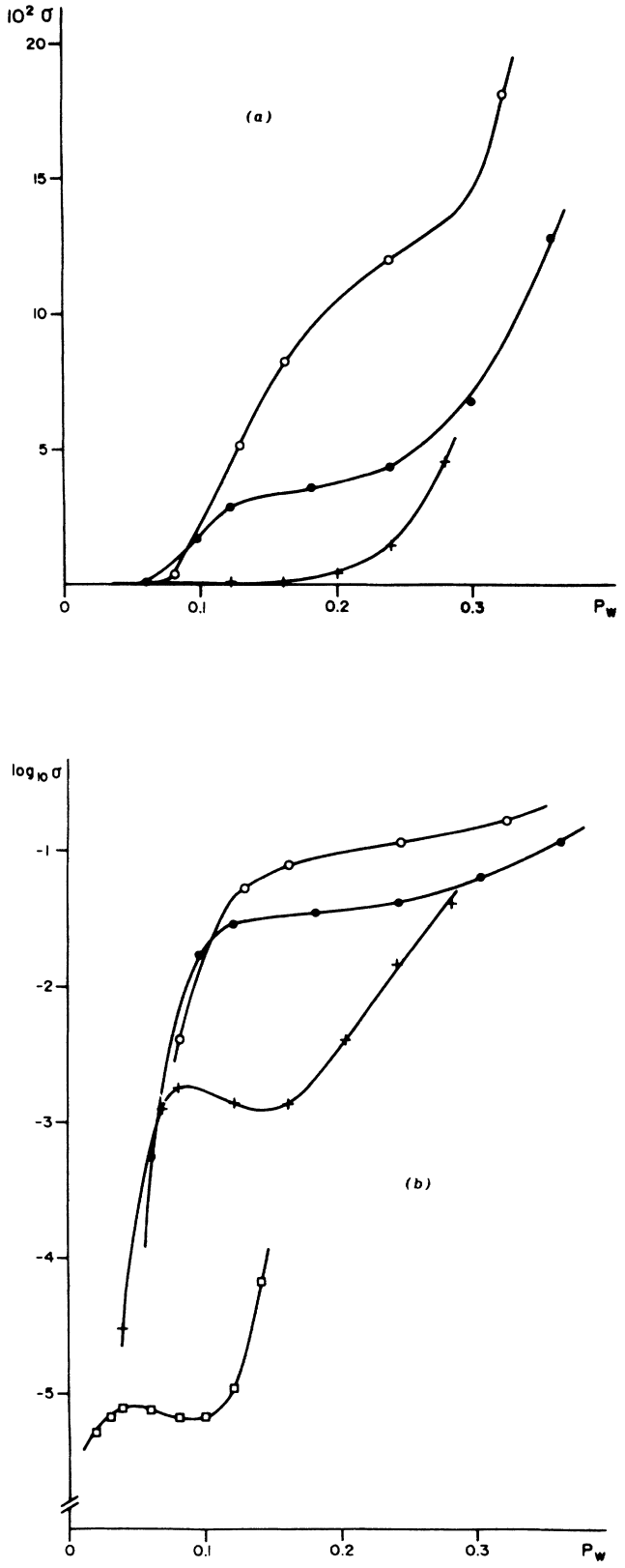

FIG. 14. Water-AOT-undecane system ($T=25\,°C$). Experimental way $P_S=$const. (□, $P_S=0.1$; +, $P_S=0.2$, ●, $P_S=0.3$; ○, $P_S=0.4$). (a) Variations of σ vs P_w; (b) Variations of $\log_{10}\sigma$ vs P_w (σ in $S\,m^{-1}$).

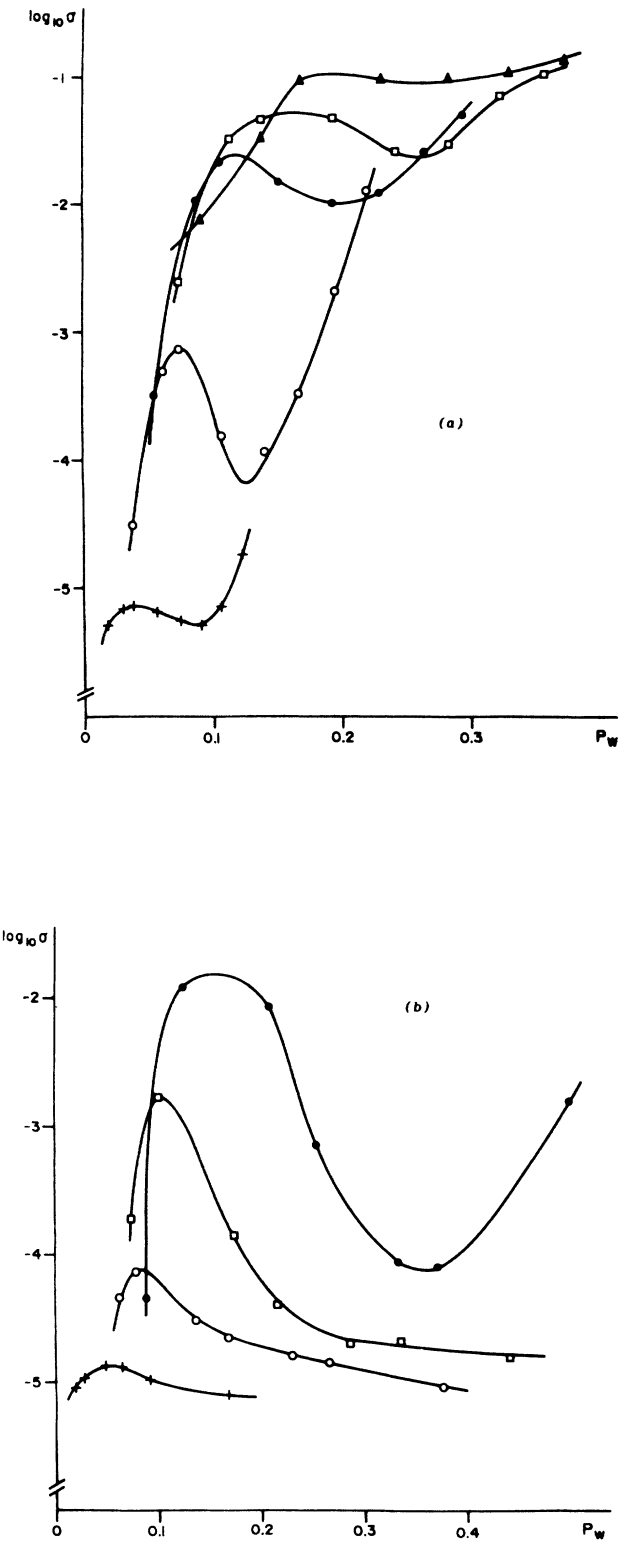

FIG. 15. Experimental way $P_S/(P_o+P_S)=$const. (a) Water-AOT-undecane system ($T=25\,°C$). Variations of $\log_{10}\sigma$ vs P_w. +, $P_S/(P_o+P_S)=0.1$; ○, $P_S/(P_o+P_S)=0.2$; ●, $P_S/(P_o+P_S)=0.3$; □, $P_S/(P_o+P_S)=0.4$; ▲, $P_S/(P_o+P_S)=0.5$; (b) Water-AOT-isooctane system ($T=25\,°C$). Variations of $\log_{10}\sigma$ vs P_w. +, $P_S/(P_o+P_S)=0.1$; ○, $P_S/(P_o+P_S)=0.3$; □, $P_S/(P_o+P_S)=0.4$; ●, $P_S/(P_o+P_S)=0.5$ (σ in $S\,m^{-1}$).

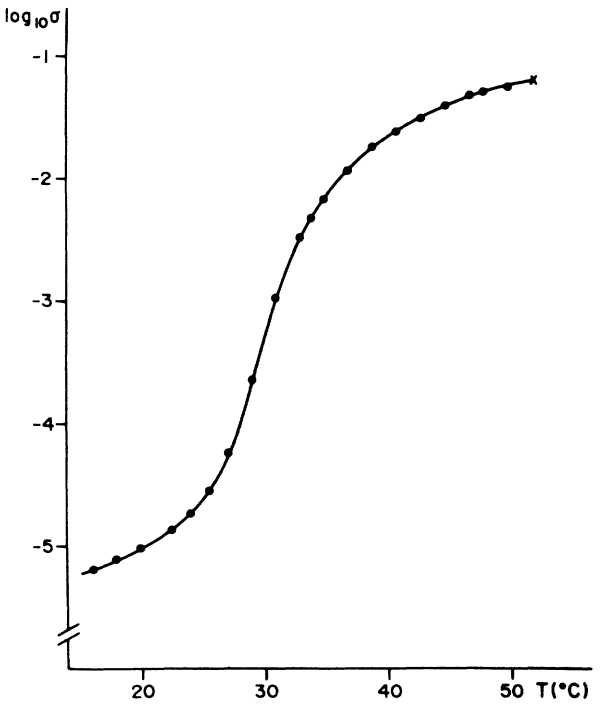

FIG. 16. Water-AOT-undecane system. Variations of the conductivity $\sigma(S\,m^{-1})$ vs temperature $T(°C)$ ($\phi=0.2$, $n=18$). (Phase separation occurs at X). (From Ref. 17).

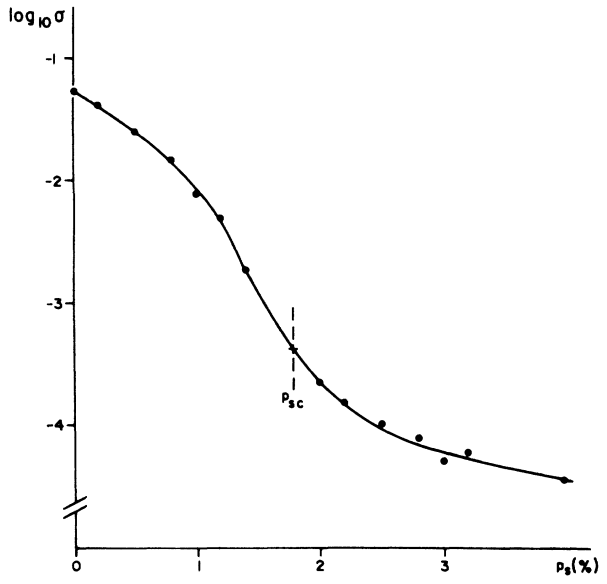

FIG. 18. Water-AOT-undecane system. Variations of the conductivity σ ($S\,m^{-1}$) vs salinity p_s (in weight percent) ($T=25\,°C$, $n=10$, $\phi=0.4$). (From Ref. 17).

are more or less pronounced. The different curves presented above keep their shape when the nature of the oil is changed. For example, Fig. 15(b) concerns the water-AOT-isooctane system. This path also correspond to $P_S/(P_S+P_o)=$const.

Path with variable temperature. Figure 16 represents the variations of $\log_{10}\sigma=f(T)$ ($\phi=0.2$, $n=8$) for the water-AOT-undecane system. For the variations of ϵ_s with temperature one can refer to the work of van Dijk *et al.*[21] for the water-AOT-isooctane system at $n=27$ for different values of the volume fraction in water ϕ_w, and hence of ϕ. The static permittivity moves through a maximum at a temperature which decreases as ϕ_w (and therefore ϕ) increases. Figure 17 is drawn from their work. For viscosity one can refer to the work of Berg, Moldover, and Huang[27] for the water-AOT-decane system. They observed an increase of the $\eta/\eta_{\text{decane}}$ ratio with increasing temperature. The same is true of water-AOT-hexane[48] system.

Variable salt content path. Figure 18 represents the variations of $\log_{10}\sigma=f(p_s)$ ($T=25\,°C$, $n=10$, $\phi=0.4$) for the (water+NACl)-AOT-undecane system. Figure 19 represents ϵ_s and the relaxation frequency ν_R as a func-

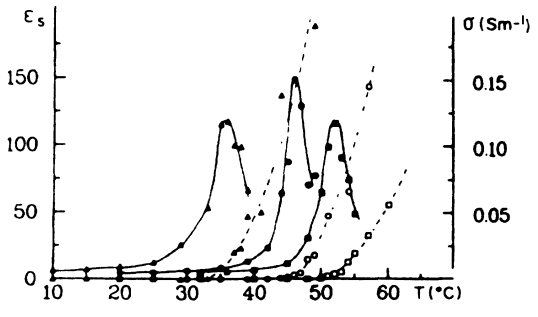

FIG. 17. Water-AOT-isooctane system ($n=27$). Variations of ϵ_s and $\sigma(S\,m^{-1})$ vs temperature of different values of ϕ_w. ▲△, 27.5%; ●○, 18.3%; ■□, 13.8% (From Ref. 20). (——) ϵ_s; (— — —) σ.

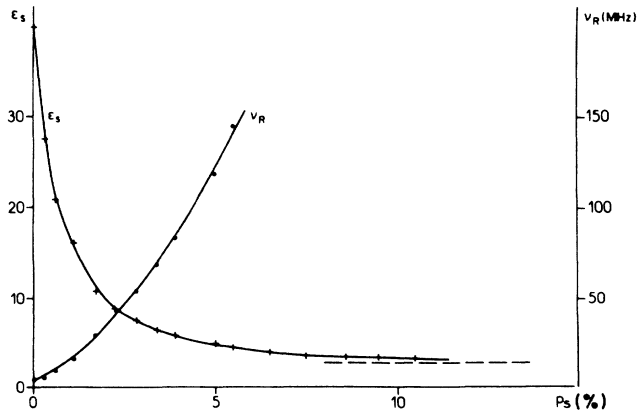

FIG. 19. Water (+NaCL)-AOT-dodecane system ($n=4.4$, $\phi=0.308$, $T=25\,°C$). Variations of ϵ_s and ν_R (MHz) vs p_s (%). (From Ref. 21).

tion of p_s for the water-AOT-dodecane system ($n=4.4$, $\phi=0.308$, $T=25\,^{\circ}C$). σ, ϵ_s, and $1/\nu_R$ decrease with increasing salt content. We observed[22] the same behavior for the water-AOT-isooctane system. For viscosity, Rouvière and co-workers[45–47] observe that the value of viscosity decreases with increasing salt content.

DISCUSSION OF THE RESULTS

Before the notion of percolation was introduced, a number of authors attempted to explain the variations of static permittivity in terms of the conventional mixing laws. This approach is still occasionally considered today. However, this interpretation comes up against the problem of the high values of ϵ_s in the neighborhood of the percolation threshold. In the framework of spherical dispersion, the maximum of ϵ_s which can be obtained, for example, with Hanai's law,[49] is given by $\epsilon_s=\epsilon_{2s}/(1-\phi)^3$ (obtained when $|\epsilon_1^*| \gg |\epsilon_2^*|$). Thus for $\phi=0.26$ and $\epsilon_{2s}\approx 2$ (static permittivity of pure oil) we have $\epsilon_s \approx 4.9$, whereas for the same volume fraction in dispersed matter we have, for undecane ($T=15\,^{\circ}C$ and $n=11$), an experimental value[50] equal to 46. Two different approaches have been used to explain this difference.

Introduction of an apparent volume fraction (Refs. 51 and 52) ϕ_a. For the previous example we would have $\phi_a=0.65$. For very high values of ϵ_s (cf. Fig. 17) the value approaches $\phi_a \approx 1$. This result is difficult to accept.

Introduction of anisotropic objects. Several authors,[50,53–55] and most recently Clarkson,[24] have envisaged the possibility that the spherical particles might form clusters, which from the dielectric point of view could be assimilated with revolution ellipsoids. Let us note at this point that to a certain extent this constitutes a simplified picture of the appearance of the conducting path in the percolation framework below the threshold (elongation of the clusters until the appearance of a cluster of infinite length). In the case of the water-AOT-dodecane system, analysis by extension of the law of Hanaï[50] to the nonspherical case leads to a maximum for ϵ_s at a high axial ratio, of the order of 9. This order of magnitude has very recently been found[24] for a quaternary system. When ϕ varies, the axial ratio moves through a maximum at the same time as ϵ_s and the calculation shows that[24,50] the relaxation frequency moves through a minimum. But while the phenomenological point of view is satisfactory, there is nothing to explain why the axial ratio goes through a maximum. Moreover, the variations with the other parameters (n, T, salt, . . .) are not explicitly analyzed.

The main criticism is that no other method is able to directly confirm this anisotropy, which is postulated in an identical way, though independently, by other authors[45–47] for viscosity. Finally, the complex shapes of the experimental curves for paths such as $P_w=\text{const}$, or $\phi=\text{const}$, etc. pose major problems of interpretation in this context.

A satisfactory theoretical model must be able to interpret both the increase of η and σ with ϕ at constant n [the derived values $(1/\eta)(d\eta/d\phi)$ and $(1/\sigma)(d\sigma/d\phi)$ must pass through a maximum] and the simultaneous passage of ϵ_s and $1/\nu_R$ (characteristic of the time of dielectric relaxation) through a maximum. It should also be able to explain the variations with T and p_s, as well as the complex shapes which correspond to the paths $P_w=\text{const}$, $P_0=\text{const}$, $P_S=\text{const}$, $P_S/P_o=\text{const}$, etc.

Our investigations[18,22,25,28] have indicated that at least for the monophase water-oil (or glycerol-oil) zone of ternary microemulsions with AOT the theory of percolation provides an overall interpretation for all the results. Figure 6 represents the values of the threshold as a function of n for different temperatures, while Fig. 20 represents the values of the threshold as a function of temperature for various values of n (water-AOT-undecane system). Figures 7(a) and 7(b) represent the corresponding threshold lines in the ternary diagram. Figure 21 represents the variations of the threshold ϕ_c with salt content.[18] These curves are sufficient to allow interpretation of all the results, if used in the context of percolation theory.

As for the variations with temperature it can be seen that there is a natural critical temperature. At $T=15\,^{\circ}C$ let us consider point B in Fig. 7(a). It corresponds to a system which is below the percolation threshold (nonconducting zone). However, at $T=25\,^{\circ}C$ it is situated above the threshold (conducting zone). At a temperature T_c between 15 °C and 25 °C point B is located on a threshold line. So the percolation transition can be observed at constant volume fraction and molar ratio when temperature varies. Moreover, Fig. 7(a) shows clearly that at constant n, T_c decreases as ϕ increases (in other words, as one moves away from the oil apex). So the curve $\epsilon_s(T)$ passes through a maximum which at $n=\text{const}$ is situationed at a temperature which decreases as the quantity of water increases, which is consistent with the experimental observations (Fig. 17). The same shape of variations has also been observed for the water-AOT-decane

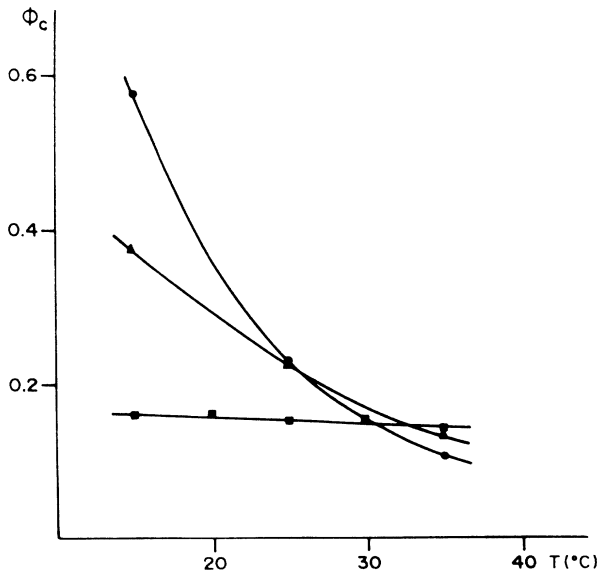

FIG. 20. Water-AOT-undecane system. Variations of the percolation threshold ϕ_c vs T. ■, $n=8$; ▲, $n=18$; ●, $n=30$. (From Ref. 17).

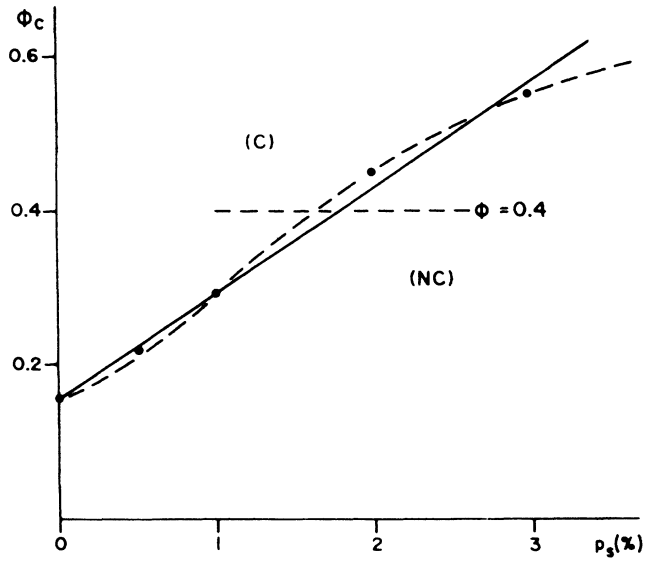

FIG. 21. Water-AOT-undecane system. Variations of the percolation threshold ϕ_c vs salinity p_s (in percent) ($n=10$, $T=25\,^{\circ}C$). (C), conductive area; (NC), nonconductive area. (From Ref. 17).

system[14] at $n=40.8$. At the same time the frequency $\nu_R(T)$ must move through a minimum which corresponds to the maximum of $\varepsilon_s(T)$. We observed this behavior in a previous study[56] for quaternary water-hexadecane-potassium oleate-hexanol–type microemulsions. This was an unusual result, which was not understood at the time.

It should be noted that the variations, for example, of σ, are given by $\sigma \propto (\phi-\phi_c)^{\mu}$ if $\phi>\phi_c$ and $\sigma \propto (\phi_c-\phi)^{-s}$ if $\phi<\phi_c$. The threshold ϕ_c at constant n depends on the temperature. If ϕ remains in the neighborhood of ϕ_c, when ϕ remains constant one can write, developing to the first order, $\phi_c(T)=\phi+K(T-T_c)$ with

$$K=\left[\frac{d\phi_c}{dT}\right]_{(T=T_c)}$$

and $\phi_c(T_c)=\phi$. If $K<0$, which corresponds to the systems presented here (Fig. 20), then $\phi>\phi_c$ if $T>T_c$. As $\sigma \propto (\phi-\phi_c)^{\mu}$ if $\phi>\phi_c$, then $\sigma \propto (T-T_c)^{\mu}$ if $T>T_c$ (when $K<0$) and similarly $\sigma \propto (T_c-T)^{-s}$ if $T<T_c$ (when $K<0$). We thus have scaling laws for temperature with the same critical exponents μ and s as for variations of ϕ. This is true if ϕ remains close to ϕ_c or if the variations of ϕ_c with T are small (for instance, value $n=8$ in Fig. 20). We checked[18] that this is also true for the value $n=18$ in Fig. 20, but it is no longer true for the value $n=30$ (except of course if ϕ remains very close to ϕ_c). In that case, the term

$$K=\left[\frac{d\phi_c}{dT}\right]_{(T=T_c)}$$

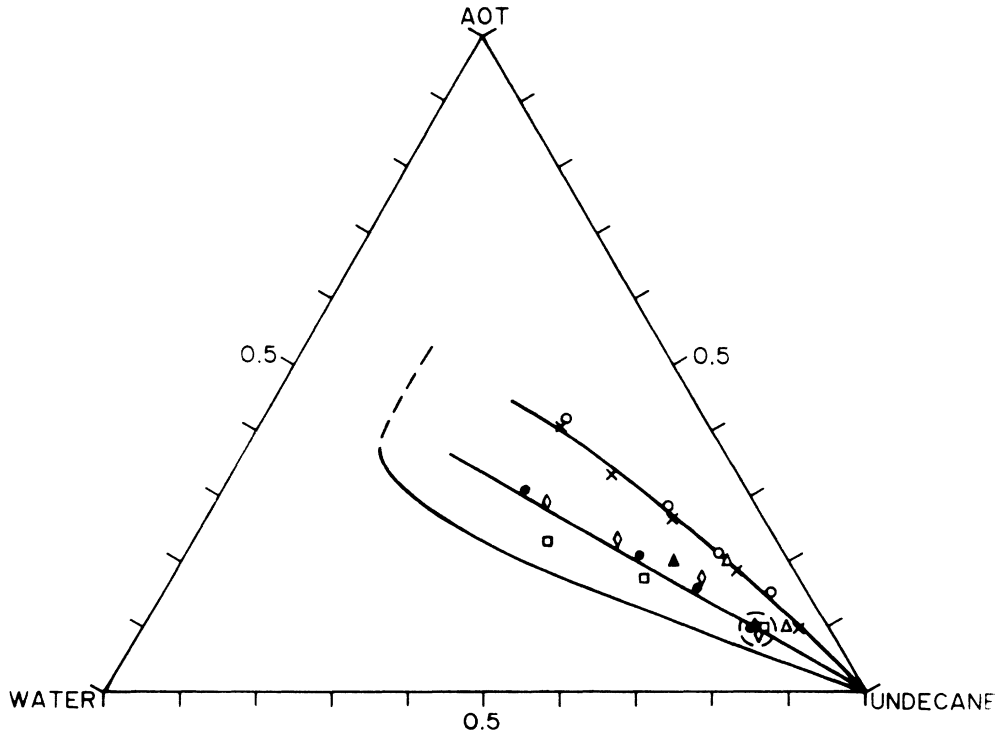

FIG. 22. Lines of the maxima and minima. Water-AOT-undecane system ($T=25\,^{\circ}C$). ×◇, Maxima and minima obtained at $P_S/(P_S+P_o)=$const; ○●, Maxima and minima obtained at $P_o=$const; ▲△, Maxima and minima obtained at $P_S=$const; □, Minima obtained at $P_w=$const.

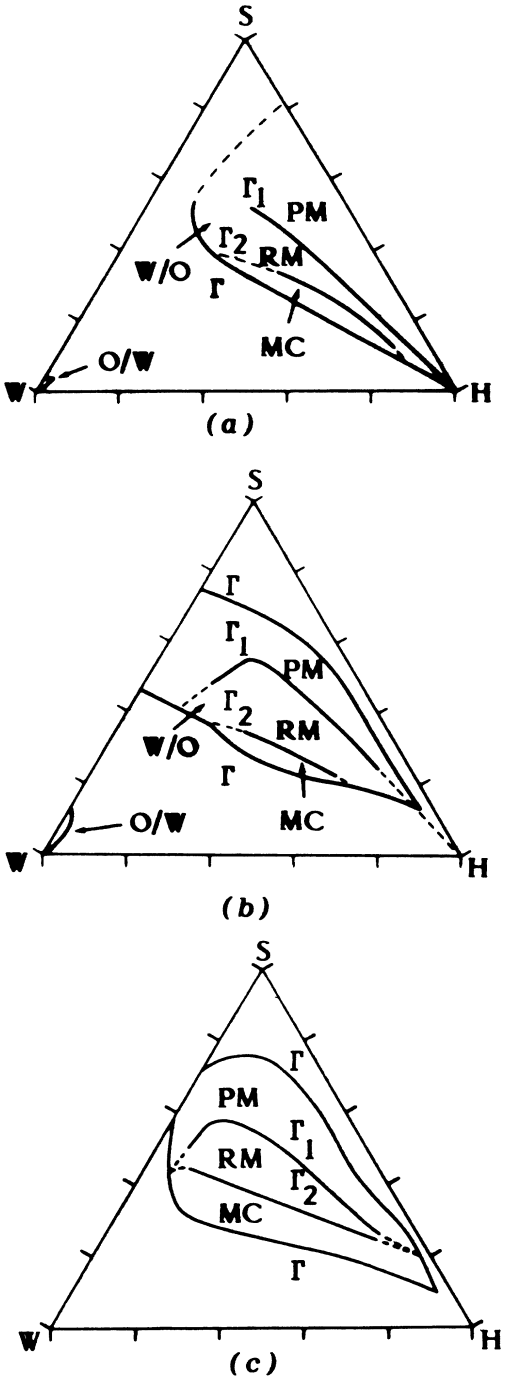

FIG. 23. Partition of the ternary diagram with the lines of "accidents." (a) *w/o* Winsor IV area in the mass ternary phase diagram of water-Aerosol OT-dodecane system at $T=298$ K. (From Ref. 31). (b) *w/o* Winsor IV area in the mass pseudoternary phase diagram of water-potassium oleate-1-pentanol-benzene systems, at $T=298$ K. *W*, 100% water; *H*, 100% hydrocarbon; *S*, 100% surface active combination (surfactant-alcohol mass ratio equal to 3/5). (From Ref. 31). (c) Pseudoternary mass phase diagram of water-hexadecane systems using potassium oleate and 1-hexanol as surface-active agents. Potassium oleate to hexanol mass ratio equal to 3/5. Curve Γ represents the border of the transparent isotropic water-in-oil type solubilization area. Temperature, $T=25$ °C. (From Ref. 32).

varies with T_c, whereas it is practically constant for $n=8$ and varies very little for $n=18$ (Fig. 20). So when $K<0$ the previous equations predict a marked increase in σ with temperature, which is experimentally observed. It should be stressed here that if $K>0$ then $\phi>\phi_c$ if $T<T_c$. So for $K>0$ we have $\sigma \propto (T-T_c)^{\mu}$ if $T<T_c$ and $\sigma \propto (T-T_c)^{-s}$ if $T>T_c$, in other words, conductivity will decrease if temperature increases. But is $K>0$ physically possible? We have indeed observed that σ decreases with temperature for the water-octylphenylether polyoxyethylene-undecane system[57] and the same behavior has recently been indicated[58] for fluorinated microemulsions, for the upper isotropic domain. However, the results reported are insufficient to verify whether these systems present the character of percolation or not. Finally, the preceding equations (with $K<0$) can be generalized to η and an increase with temperature does occur as we have indicated. But as the prefactor values change with temperature [for example, $C_1\sigma_1(T)$ in Eq. (5)

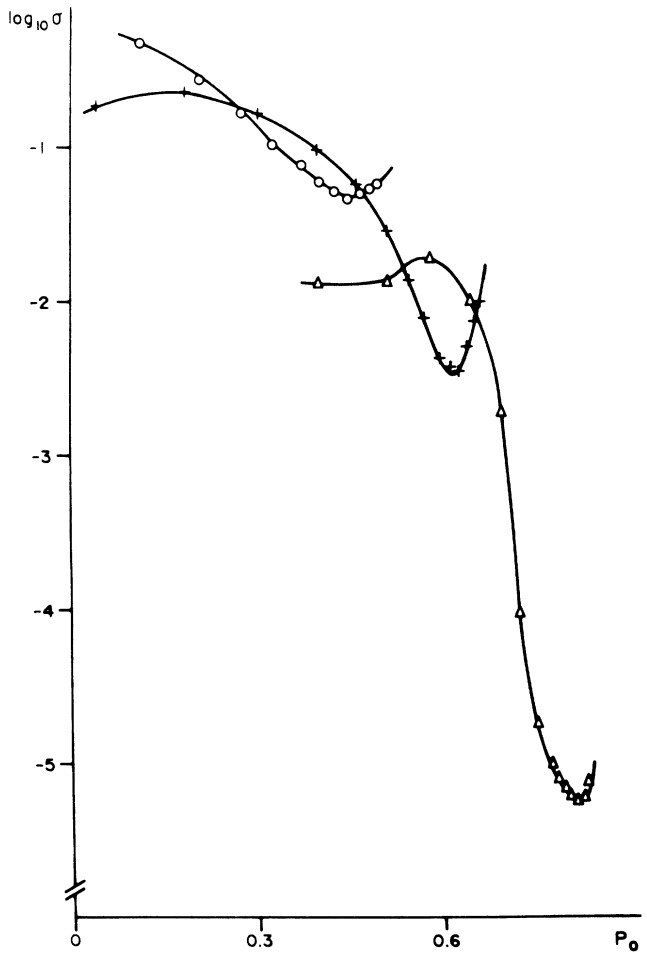

FIG. 24. Water-AOT-undecane system ($T=25$ °C). Experimental way $P_w=$const. Theoretical reconstitution. Variations of $\log_{10}\sigma$ (○, $P_w=0.3$; +; $P_w=0.2$; △, $P_w=0.1$) vs P_o. (σ in $S\,m^{-1}$).

and $C_1'' \eta_1(T)$ in Eq. (8)] it is in fact necessary to consider the ratio $\sigma(T)/\sigma_1(T)$ or $\eta(T)/\eta_1(T)$. For instance, the viscosity of glycerol decreases very sharply as temperature increases, so the increase due to the percolation effect is hidden and the viscosity of the microemulsion decreases, whereas the ratio $\eta(T)/\eta_1(T)$ increases.[64]

Figure 21, which represents the variation of the threshold ϕ_c with the salt content p_s for the water-AOT-undecane system ($T=25°$ C, $n=10$), can be discussed in a similar way. It is clearly apparent that at constant ϕ ($\phi=0.4$ for Fig. 18), when p_s is low, ϕ is greater than ϕ_c, and we are in the conducting zone. If p_s increases, $|\phi-\phi_c|$ decreases in the conducting zone and conductivity decreases. If p_s has the particular value p_{sc} one obtains $\phi_c(p_{sc})=\phi$. Then, if p_s continues to increase, $|\phi-\phi_c(p_{sc})|$ increases in the nonconducting zone and σ continues to decrease. As above, one can write $\phi_c(p_s)=\phi+K(p_s-p_{sc})$ with

$$K=\left[\frac{d\phi_c}{dp_s}\right]_{(p_s=p_{sc})}>0 .$$

This means that $\sigma \propto |p_s-p_{sc}|^{\mu}$ if $p_s<p_{sc}$ and $\sigma \propto |p_s-p_{sc}|^{-s}$ if $p_s>p_{sc}(\phi<\phi_c)$. These relations clearly predict a decrease in σ when p_s increases, with passage through a percolation threshold for $p_s=p_{sc}$ (Fig. 18). By the same reasoning one can understand why for viscosity η, at constant n and ϕ, the viscosity decreases with increasing salt content.[45–47]

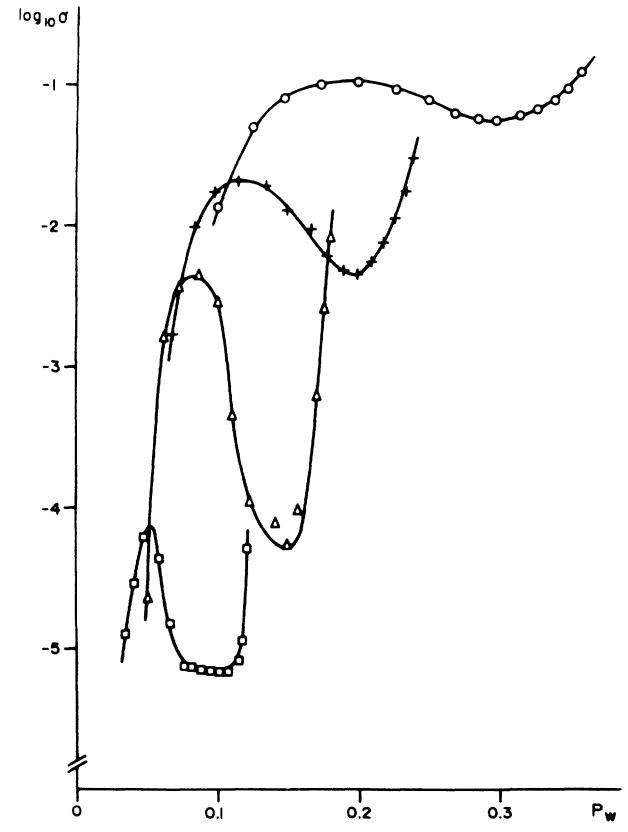

FIG. 25. Water-AOT-undecane system ($T=25$ °C). Experimental way $P_o=$const. Theoretical reconstitution. Variations of $\log_{10}\sigma$ (○, $P_o=0.4$; +, $P_o=0.6$; △, $P_o=0.7$; □, $p_o=0.8$) vs P_w. (σ in S m^{-1}).

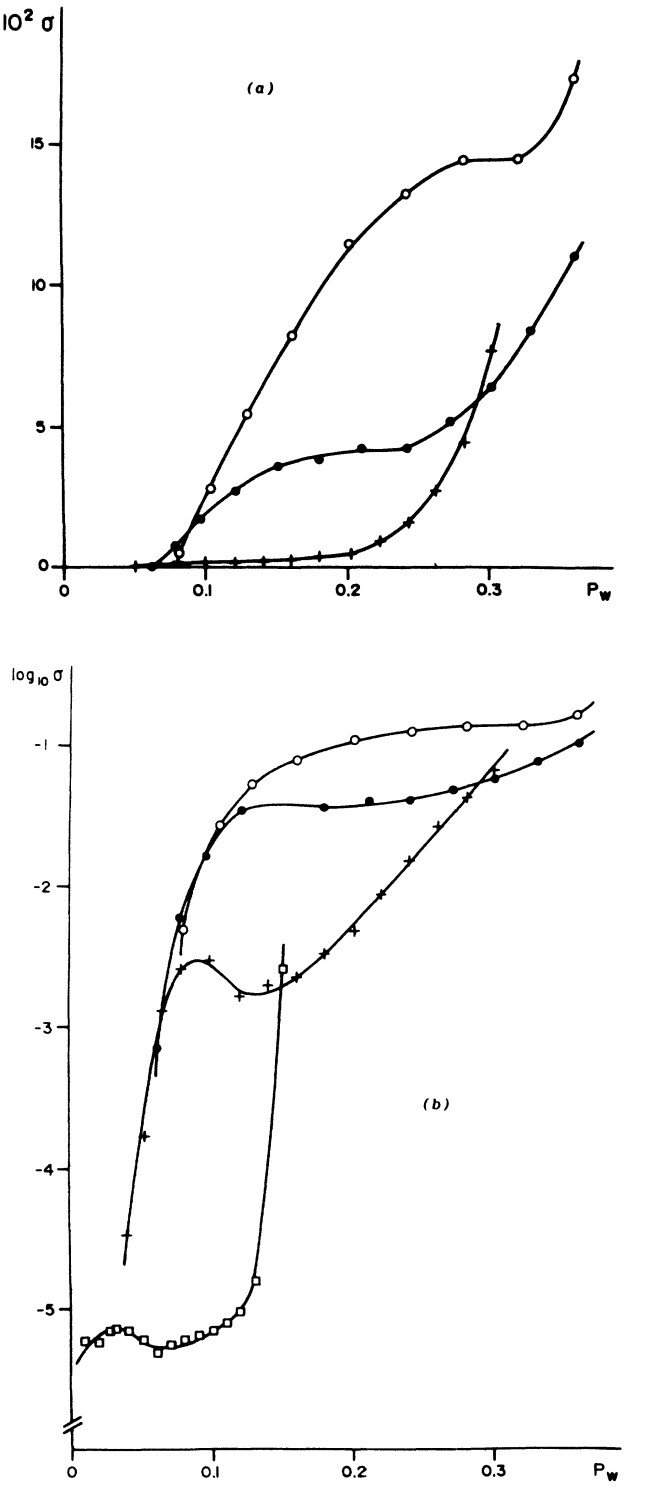

FIG. 26. Water-AOT-undecane system ($T=25$ °C). Experimental way $P_S=$const. Theoretical reconstitution. (□, $P_S=0.1$; +, $P_S=0.2$; ●, $P_S=0.3$; ○, $P_S=0.4$). (a) Variations of σ vs P_w; (b) Variations of $\log_{10}\sigma$ vs P_w (σ in S m^{-1}).

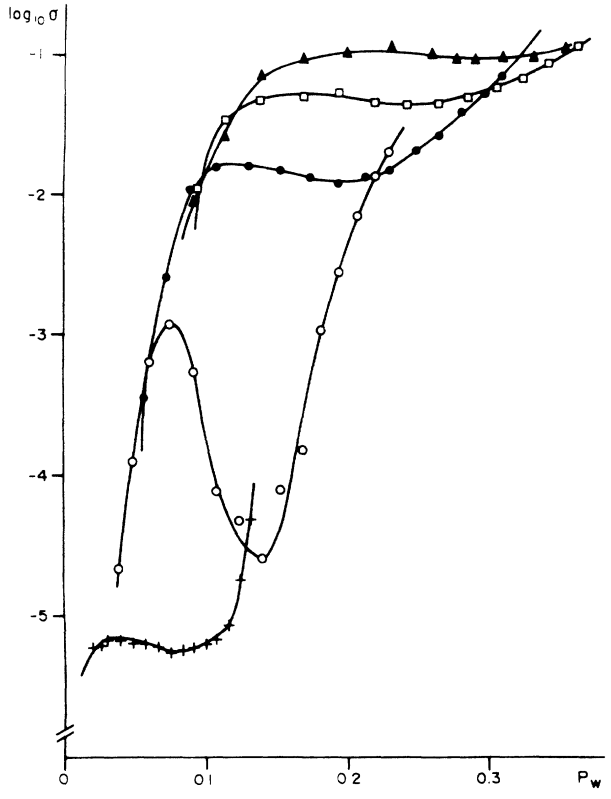

FIG. 27. Water-AOT-undecane system ($T=25\,°C$). Experimental way $P_S/(P_o+P_S)=$const. Variations of $\log_{10}\sigma$ vs P_w (+, 0.10; ○, 0.2; ●, 0.3; □, 0.4; ▲, 0.5) (σ in S m^{-1}).

The measurements carried out at constant ϕ, T, and p_s and variable n show maxima and minima for ϵ_s,σ, and η, according to the experimental conditions. These variations can be explained by the corresponding variations of $|\phi-\phi_c(n)|$. Figures 9, 10, and 11 are characteristic. The maxima and minima do not correspond to structural changes but are simply linked to the "distance" $|\phi-\phi_c|$ at the threshold, given the variation curve $\phi_c(n)$. Let us now consider the path B_1B_2 which corresponds to $P_S/P_o=$const. When the water content, i.e., P_w, increases, n also increases. At $T=15\,°C$ the point B_1 is in the conducting region. When water is added the microemulsion moves into the nonconducting region after having crossed the threshold line corresponding to $T=15\,°C$. Thus on the experimental path the addition of water causes σ to decrease, while on the path $n=$const the addition of water leads to an increase in σ. On the path B_1B_2 the addition of water also causes a reduction in viscosity. If, instead of starting out from point B_1, one sets out from a point located on the AOT-oil side, moving with $P_S/P_o=$const (Fig. 8) towards the water apex at $T=15\,°C$, one will move from the nonconducting zone (NC) to the conducting zone (C), then from the conducting zone (C) back to the nonconducting zone (NC), which means that conductivity and viscosity will first increase[59–62] and then decrease.

We will now show that a brief analysis of the results obtained on the paths which at $T=$const and $p_s=$const do not correspond to $n=$const (in other words, which do not keep a constant interaction between droplets) can

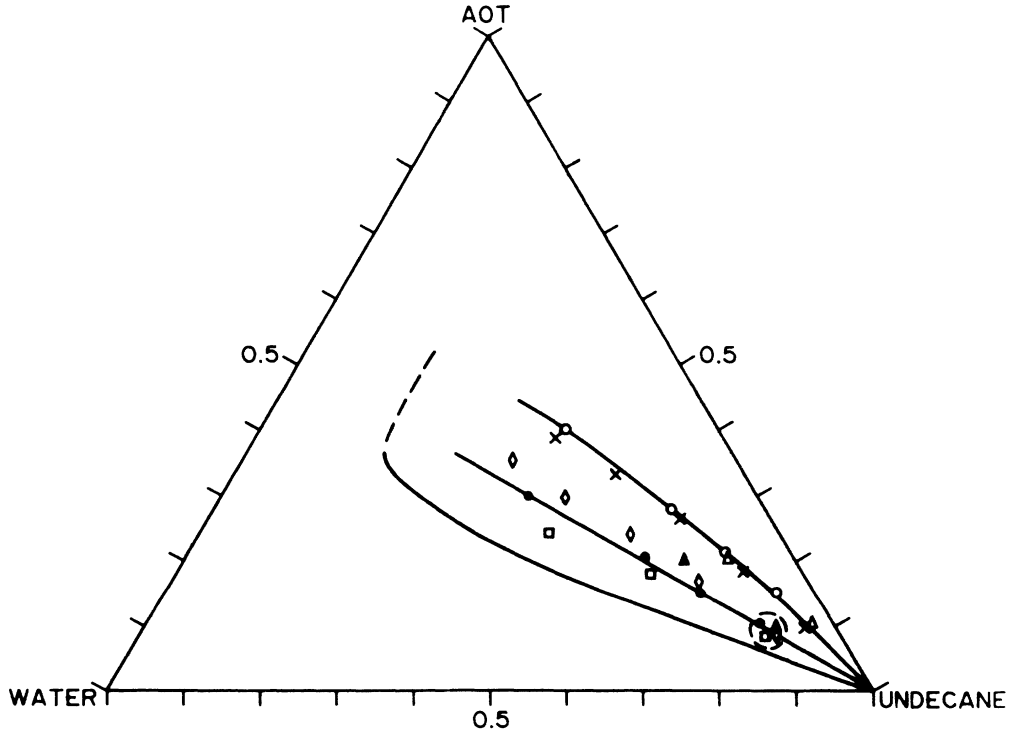

FIG. 28. Lines of the maxima and minima. Water-AOT-undecane system ($T=25\,°C$). ×◇, Maxima and minima obtained at $P_S/(P_S+P_o)=$const; ○●, Maxima and minima obtained at $P_o=$const; ▲△, Maxima and minima obtained at $P_S=$const; □, Minima obtained at $P_w=$const; (——, Solid lines from Fig. 22).

yield incorrect interpretation. The position of the maxima and minima observed in Figs. 12–15 correspond to points in the ternary diagram which allow two lines, representative of these "accidents," to be plotted. The ternary diagram is consequently divided into three zones (Fig. 22). In previous investigations, we divided the diagram in this way for the water-AOT-dodecane system,[32] and also[31–34] for several quaternary systems such as water-potassium oleate-hexanol-hexadecane, for example, (Fig. 23) in the monophase water-oil zone. At the time, we indicated that the zone which contained the least water was the premicellar zone (zone PM), followed by the reverse micelles zone (zone RM), then by a zone of clustering (zone MC). In this analysis, the crossing of the two lines of "accidents" corresponds to a structural change. Only the zone (MC) involves the phenomenon of clustering, which is the basis of microemulsion percolation but the idea of percolation was not even mentioned. In the context of interpretation in terms of percolation there are no structural changes and clustering occurs, to varying degrees, throughout the phase diagram. The shapes of the experimental curves depend simply, as we have already indicated, on the distance $|\phi-\phi_c|$ at the threshold, and thus on the shape of variations of ϕ_c, which should be connected with the interactions in the system.[22] For the water-AOT-undecane system, we generated curves calculated by computer for various experimental paths, using the experimental values of $\phi_c(n)$ indicated in Ref. 63, or read from the curves of Fig. 6. We used $\sigma=A(\phi_c-\phi)^{-1.2}$ if $\phi<\phi_c$ and $\sigma=B(\phi-\phi_c)^{1.94}$ if $\phi>\phi_c$ with $\log_{10}A=-6.5$ and $\log_{10}B=-0.28$, which are average deduced values.[18,63] Figs. 24–27 provide a few-examples which can be compared with the experimental Figs. 12–15. At the maxima and minima correspond to course two lines in the ternary diagram (Fig. 28), similar to those in Fig. 22 and 23. The quantitative agreement is not rigorous because we used the average values for A and B. However, this does show clearly that it is the shape of the curve $\phi_c(n)$ which predominates. Together, the curves calculated show that the qualitative interpretation that was previously put forward is not justified and that percolation theory is sufficient to account for all the results.

CONCLUSIONS

The simultaneous variations of conductivity, dielectric relaxation, and dynamic viscosity can be interpreted, at least qualitatively, within the framework of percolation theory. For ternary systems of the water(glycerol)-AOT-oil type, the variations of these quantities as a function of the volume fraction in dispersed matter, of temperature, and of the salt content, as well as variations with respect to the molar ratio, are easily interpreted. Certain curious results obtained by other authors and reported above can be more clearly interpreted in the context of this theory. The accidents (maxima and minima) obtained on the curves of viscosity, conductivity, and static permittivity are linked to the experimental path followed. They would not be interpreted by invoking structural changes (division of the monophase zone into three regions of different structures), or the presence of more or less elongated ellipsoids, nor any other factor whose sole purpose is to provide, through adjustment, qualitative or quantitative agreement on one single aspect of the behavior of the system.

The behavior of these systems only depends on the distance $(\phi-\phi_c)$ of the representative point on the ternary diagram (characterized by ϕ and n), at the value of the threshold at the same temperature, which depends on interaction within the system. Consequently, the most convenient experimental path is that which maintains a constant interaction. At fixed temperature and salt content, this is the path $n=$const. For all the other paths, within the term $(\phi-\phi_c)$, the value of ϕ_c varies at each point on the path. It is therefore possible to move through a percolation point, in other words, to be at a point on the threshold line without realizing it, which naturally makes correct analysis of the experimental curve very difficult.

These remarks valid for systems of the water(glycerol)-AOT-oil type appear to apply equally to quaternary systems, at least to those in which the monophase water-oil zone is separated from the monophase oil-water zone ("S"-type systems, according to the terminology we have suggested[34]). However, in this case the experimental path at a constant interaction does not correspond to the path $P_w/P_s=$const [Fig. 8(b)] because of the presence of alcohol. Generally, in the phase tetrahedron the constant interaction path is not located in a plane such that $P_S/P_{\text{alcohol}}=$const. It crosses several such planes. It is nonetheless easy to follow a line at a constant interaction for a quaternary system by operating by dilution based on points located on the demixing line. Preliminary studies[64] provide curves which can indeed be analyzed on the basis of percolation theory. As a general rule a systematic analysis has to be carried out in the phase tetrahedron at each temperature, as a function of the volume fraction in dispersed matter and of the different molar ratios. The important parameter is the percolation threshold and one needs to know the position within the phase tetrahedron of the threshold which corresponds to a given interaction. While we have been able to define the threshold line for ternary systems, it is probable that for quaternary systems it will be necessary to define the "threshold surface" in the phase tetrahedron.

To conclude, it should be emphasized that on the basis of these results, it is clearly essential to identify the percolating or nonpercolating nature of the system studied. If the system is of a "percolating" nature, the position of any "accidents" (maxima and minima) which might appear must be studied in relation to the percolation threshold line. If this is not done, then there is a risk that misleading conclusions might be drawn.

[1]G. J. Smith, C. E. Donelan, and R. E. Barden, J. Colloid Interface Sci. **60**, 488 (1977).
[2]Y. L. Khmelnitsky, R. Hilhorst, and C. Veeger, Eur. J. Biochem. **176**, 265 (1988).
[3]I. Rico and A. Lattes, Nouv. J. Chim. **8**, 429 (1984).
[4]B. Pouligny, J. R. Lalanne, B. Couillaud, A. Ducasse, and L. Sarger, Opt. Commun. **37**, 271 (1981).
[5]P. D. I. Fletcher, B. H. Robinson, and J. Tabony, J. Chem. Soc. Faraday Trans. 1 **82**, 2311 (1986).
[6]K. P. Das, A. Ceglie, and B. Lindman, J. Phys. Chem. **91**, 2938 (1987).
[7]S. E. Friberg and Y. C. Liang, Colloids Surf. **24**, 325 (1987).
[8]M. Lagues, R. Ober, and C. Taupin, J. Phys. Lett. (Paris) **39**, L487 (1978).
[9]B. Lagourette, J. Peyrelasse, C. Boned, and M. Clausse, Nature (London) **281**, 60 (1979).
[10]M. Lagues, J. Phys. Lett. (Paris) **40**, L331 (1979).
[11]M. Lagues and C. Sauterey, J. Phys. Chem. **84**, 3503 (1980).
[12]A. M. Cazabat, D. Chatenay, D. Langevin, and J. Meunier, Faraday Discuss. Chem. Soc. **76**, 291 (1982).
[13]M. A. Van Dijk, Phys. Rev. Lett. **55**, 1003 (1985).
[14]S. Bhattacharya, J. P. Stokes, M. W. Kim, and J. S. Huang, Phys. Rev. Lett. **55**, 1184 (1985).
[15]D. Chatenay, W. Urbach, A. M. Cazabat, and D. Langevin, Phys. Rev. Lett. **54**, 2253 (1985).
[16]D. Beaglehole and M. T. Clarkson, in *Localization and Metal Insulator Transitions,* edited by H. Fritzsche and D. Adler (Plenum, New York, 1985), p. 153.
[17]M. W. Kim, and J. S. Huang, Phys. Rev. A **34**, 719 (1986).
[18]M. Moha-Ouchane, J. Peyrelasse, and C. Boned, Phys. Rev. A **35**, 3027 (1987).
[19]G. S. Grest, J. Webman, S. A. Safran, and A. L. R. Bug, Phys. Rev. A **33**, 2842 (1986).
[20]S. A. Safran, J. Webman, and G. S. Grest, Phys. Rev. A **32**, 506 (1985).
[21]M. A. Van Dijk, G. Casteleijn, J. G. H. Joosten, and Y. K. Levine, J. Chem. Phys. **85**, 626 (1986).
[22]J. Peyrelasse, M. Moha-Ouchane, and C. Boned, Phys. Rev. A **38**, 904 (1988).
[23]M. T. Clarkson and S. I. Smedley, Phys. Rev. A **37**, 2070 (1988).
[24]M. T. Clarkson, Phys. Rev. A **37**, 2079 (1988).
[25]J. Peyrelasse, C. Boned, and Z. Saidi, Proceedings of the Second European Colloid and Interface Society Conference, Bordeaux-Arcahon, 1988 [Prog. Colloid Polym. Sci. **79**, 263 (1989)].
[26]I. Rico and A. Lattes, J. Colloid Interface Sci. **102**, 285 (1984).
[27]R. F. Berg, M. R. Moldover, and J. S. Huang, J. Chem. Phys. **87**, 3687 (1987).
[28]J. Peyrelasse, M. Moha-Ouchane, and C. Boned, Phys. Rev. A **38**, 4155 (1988).
[29]M. Borkovec, H. F. Eicke, H. Hammerich, and B. Das Gupta, J. Phys. Chem. **92**, 206 (1988).
[30]D. Quemada and D. Langevin, J. Theor. Appl. Mech. (Numero Spécial) 201 (1985).
[31]C. Boned, M. Clausse, B. Lagourette, J. Peyrelasse, V. E. R. Mc Clean, and R. J. Sheppard, J. Phys. Chem. **84**, 1520 (1980).
[32]C. Boned, J. Peyrelasse, J. Heil, M. Zradba, and M. Clausse, J. Colloid Interface Sci. **88**, 602 (1982).
[33]M. Clausse, C. Boned, J. Peyrelasse, B. Lagourette, V. E. R. Mc Clean, and R. J. Sheppard, in *Surface Phenomena in Enhanced Oil Recovery,* edited by D. O. Shah (Plenum, New York, 1981), p. 199.
[34]M. Clausse, J. Peyrelasse, C. Boned, J. Heil, L. Nicolas-Morgantini, and A. Zradba, in *Surfactants in Solutions,* edited by K. L. Mittal and B. Lindman (Plenum, New York, 1984), Vol. 3, p. 1583.
[35]A. L. Efros and B. L. Shklovskii, Phys. Stat. Sol. **76B**, 475 (1976).
[36]D. Stroud and J. Bergman, Phys. Rev. B **25**, 2061 (1982).
[37]L. Benguigui, J. Yacubowicz, and M. Narkis, J. Polym. Sci. B **25**, 127 (1987).
[38]L. Benguigui, J. Phys. Lett. (Paris) **46**, L1015 (1985).
[39]J. Peyrelasse, C. Boned, and J. P. le Petit, J. Phys. E **14**, 1002 (1981).
[40]C. Boned and J. Peyrelasse, J. Phys. E **15**, 534 (1982).
[41]J. S. Huang, S. A. Safran, M. W. Kim, G. S. Grest, M. Kotlarchyk, and N. Quirke, Phys. Rev. Lett. **53**, 592 (1984).
[42]M. J. Hou, M. Kim, and D. O. Shah, J. Colloid Interface Sci. **123**, 398 (1988).
[43]P. D. I. Fletcher, M. F. Galal, and B. H. Robinson, J. Chem. Soc. Faraday Trans. 1 **80**, 3307 (1984).
[44]A. L. R. Bug, A. Safran, G. S. Grest, and I. Webman, Phys. Rev. Lett. **55**, 1896 (1985).
[45]J. Rouviere, J. M. Couret, R. Marrony, and J. L. Dejardin, C. R. Acad. Sci. (Paris) **286C**, 5 (1978).
[46]J. Rouviere, J. M. Couret, A. Lindheimer, M. Lindheimer, and B. Brun, J. Chim. Phys. **76**, 297 (1979).
[47]J. Rouviere, J. M. Couret, M. Lindheimer, J. L. Dejardin, and R. Marrony, J. Chim. Phys. **76**, 289 (1979).
[48]H. F. Eicke, R. Hilfiker, and M. Holz, Helv. Chim. Acta **67**, 361 (1984).
[49]T. Hanai, Kolloid Z. Z. Polym. **71**, 23 (1960).
[50]J. Peyrelasse and C. Boned, J. Phys. Chem. **89**, 370 (1985).
[51]R. H. Cole, G. Delbos, P. Winsor, T. K. Bose, and J. M. Moreau, J. Phys. Chem. **89**, 3338 (1985).
[52]H. F. Eicke, S. Geiger, F. A. Sauer, and H. Thomas, Ber. Bunsenges. Phys. Chem. **90**, 872 (1986).
[53]J. Sjoblom, B. Jonsson, C. Nylander, and L. Lundstrom, J. Coll. Int. Sci. **100**, 27 (1984).
[54]R. Henze and U. Schreiber, Ber. Bunsenges. Phys. Chem. **88**, 1075 (1984).
[55]R. Henze and U. Schreiber, Colloid Polym. Sci. **263**, 164 (1985).
[56]J. Peyrelasse, V. E. R. Mc Clean, C. Boned, R. J. Sheppard, and M. Clausse, J. Phys. D **11**, L117 (1978).
[57]J. Peyrelasse, C. Boned, P. Xans, and M. Clausse, in *Emulsions, Lattices and Dispersions,* edited by P. Becher and M. N. Yudenfreund (Marcel Dekker, New York, 1979), p. 221.
[58]C. Burger-Guerrissi, C. Tondre, and D. Canet, J. Phys. Chem. **92**, 4974 (1988).
[59]J. Chen, D. F. Evans, B. W. Ninham, D. O. J. Mitchell, F. D. Blum, and S. Pickup, J. Phys. Chem. **90**, 842 (1986).
[60]J. Chen, D. F. Evans, and B. W. Ninham, J. Phys. Chem. **88**, 1631 (1984).
[61]J. Chen, D. F. Evans, and B. W. Ninham, J. Phys. Chem. **91**, 1823 (1987).
[62]B. W. Ninham, I. S. Barnes, S. T. Hyde, P. J. Derian, and T. N. Zemb, Europhys. Lett. **4**, 561 (1987).
[63]M. Moha-Ouchane, Thèse de Doctorat, Université de Pau, 1987.
[64]J. Peyrelasse, Z. Saidi, and C. Boned (unpublished).

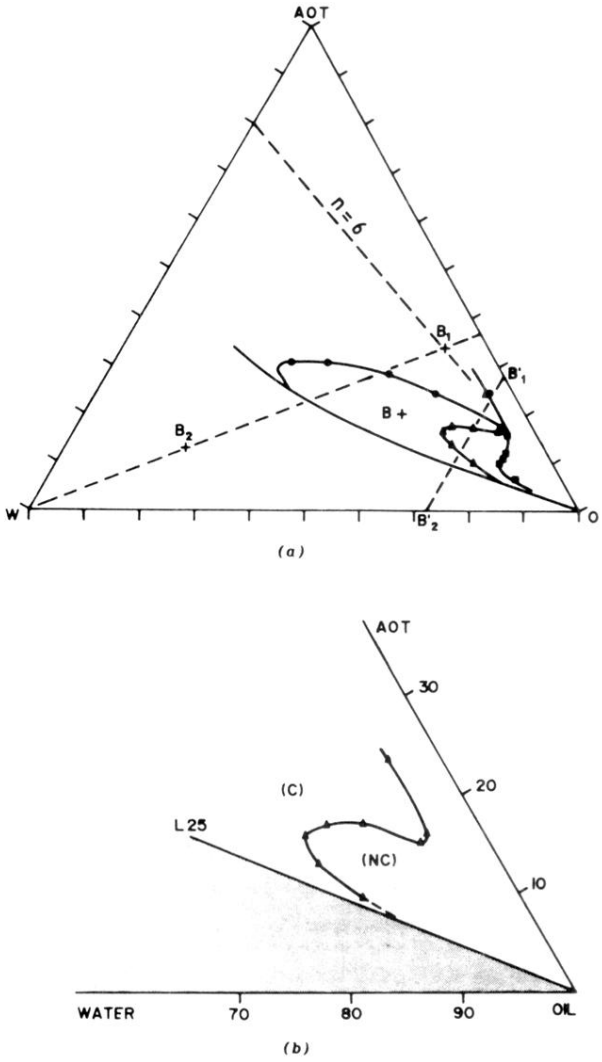

FIG. 7. Water-AOT-undecane system. (From Ref. 17). (a) Lines of the percolation thresholds in the ternary diagram (weight fraction). ●, $T=15$°C; ▲, $T=25$ °C; ■, $T=35$ °C; (b) Line of the percolation thresholds in the ternary diagram (weight fraction) at $T=25$ °C. L25, boundary of the monophasic area at $T=25$ °C. (C), conductive area; (NC), nonconductive area.